

# Reduced-pressure foaming of aluminium alloys

G. S. Vinod Kumar<sup>\*1,2</sup>, M. Mukherjee<sup>1,2</sup>, F. Garcia-Moreno<sup>1,2</sup>, J. Banhart<sup>1,2</sup>

<sup>1</sup>Technische Universität Berlin, Hardenbergstraße 36, 10623 Berlin, Germany

<sup>2</sup>Helmholtz-Zentrum Berlin für Materialien und Energie, Hahn-Meitner-Platz 1, 14109 Berlin, Germany

## Abstract

We developed a novel process for foaming aluminium and its alloys without using a blowing agent. The process involves a designated apparatus in which molten aluminium and its alloys are first foamed under reduced pressure and then solidified quickly. Foaming was done for pure aluminium (99.99%) and AlMg5 alloy not containing stabilizing particles and AlMg5 and AlSi9Mg5 alloys containing 5 vol.% of SiO<sub>2</sub> particles. We discuss the foaming mechanism and develop a model for estimating the porosity that can be achieved in this process. The nucleation of pores in foams is also discussed.

**Keywords:** Aluminium foams, Reduced pressure test (RPT), Foam stabilisation, Sievert's law, Hydrogen porosity

## 1. Introduction

The process of making closed cell aluminium alloy foams directly from liquid metal alloys involves gas that is obtained either by the decomposition of blowing agent powders such as TiH<sub>2</sub> [1-3,4] or CaCO<sub>3</sub> [5,6] that are admixed to the liquid metal, or is based on directly injected gases, usually air, nitrogen or argon [7,8]. TiH<sub>2</sub> is the most frequently used blowing agent for foaming aluminium alloys and decomposes inside

---

\* Contact: [vinodnarasimha@gmail.com](mailto:vinodnarasimha@gmail.com)

the melt while releasing hydrogen gas that forms the bubbles. Gasar <sup>[9]</sup> or Lotus <sup>[10]</sup> materials are made by foaming molten metals without using blowing agents or injecting gas but rather by melting and solidifying metals under partial gas pressure. During solidification, dissolved gas is partially rejected by the melt and forms directional or radial pores in the metallic matrix. Every metal and alloy that dissolves gas is amenable to this method. Aluminium responds rather poorly to this process due to its low hydrogen solubility in the molten state in comparison to other metals <sup>[10]</sup>. Still, aluminium and its alloys can pick up from the ambient atmosphere and dissolve in the melt enough hydrogen gas to create some porosity during solidification, during which part of this hydrogen is rejected from the solid-liquid interfaces due to the pronounced jump of gas solubility. Gas volume fractions are low in this case and depend on the liquid solubility as a function of temperature <sup>[11]</sup> and alloying elements <sup>[12,13]</sup>. Foundries study porosities by applying the *reduced-pressure test* (RPT), also known as the Straube–Pfeiffer technique, to quantify the dissolved hydrogen <sup>[14]</sup>. Molten aluminum alloy is poured into a pressure-tight chamber under normal pressure and is then allowed to expand under reduced pressure, usually in the range of 60 to 130 mbar, after which the alloy is finally solidified <sup>[14]</sup>. The growth of porosity is promoted by the pressure drop and the amount of porosity that is created by a given amount of hydrogen gas and is much larger compared with what is obtained under isobaric casting conditions. The gas porosity is governed by the gas law, i.e. the volume of the gas is inversely related to the pressure applied. As an example, the pore fraction is increased by a factor of 10 when the melt initially held at 1 bar pressure is solidified under 100 mbar pressure <sup>[11]</sup>.

Renger and Kaufmann <sup>[15]</sup> used a reduced-pressure apparatus to foam molten magnesium alloy scrap that contained large amounts of both dissolved hydrogen and

oxides, the latter increasing melt viscosity and ensuring foam stability. Wiehler et al. [16] have shown the possibility of foaming under reduced pressure a AlSi9Cu alloy containing dissolved hydrogen gas. The pressure drop was achieved by mould expansion and the cold mould wall ensured fast solidification of the foams.

We developed and applied a reduced-pressure foaming (RPF) apparatus in an analogous way to the RPT and foamed aluminium and aluminium alloys by expanding the volume of nucleated hydrogen under reduced pressure. The apparatus was designed to obtain a quick pressure reduction and to solidify the foams quickly.

## **2. Experimental details**

### *2.1 Reduced-pressure foaming apparatus*

Figure 1 shows the schematic of the reduced-pressure foaming (RPF) apparatus. Foaming is performed in a horizontal cylindrical steel tube of  $\phi$  20 mm and 120 mm length with a 5-mm thick wall. The foaming tube is connected to a vacuum pump at one end and to a water cooled copper ladle acting as a melt reservoir on the other. The copper ladle has an orifice at the bottom and a steel funnel at the top. All connections are maintained air-tight to achieve a quick pressure reduction. A wire mesh in the connection to the rotary pump helps protecting the pump from possible overflows of the molten metal or foam.

### *2.2 Foaming Procedure*

150 g of Al alloy is melted in a vertical resistance furnace at the desired superheat of 100 to 200 K above the alloy's melting point. The melt is isothermally held for 2 to 3 hours and intermittently skimmed to remove the surface oxide, thus enhancing hydrogen pickup from the surrounding atmosphere. In some cases, the melt is stirred

for 20 minutes during which stabilizing particles are added. While the rotary vacuum pump of the RPF apparatus is already running the melt is poured through the funnel into the copper ladle. Immediately after the melt has filled the funnel and thereby seals the system a pressure drop is generated by opening the valve. The melt is sucked into the foaming tube where it immediately starts to foam under the reduced pressure and eventually fills the tube. The residual melt (about 25% of the original quantity) solidifies inside the copper ladle and thereby closes the system and maintains the reduced pressure inside the tube. The liquid foam cools at a rate of on average 35 K/s as measured inside the foaming tube with a K-type thermocouple and eventually solidifies.

Foaming was carried out for pure aluminium (99.99%) and AlMg5 alloy which were melted and held isothermally at 850 °C and 750 °C respectively. AlMg5 and AlSi9Mg alloys containing 5 vol.% of SiO<sub>2</sub> particles (average size 44 μm) were also tested for foaming. The details of foaming parameters are given in Table 1.

### *2.3 Structural analysis*

X-ray tomography of the foams was performed with a μCT setup composed of a microfocus X-ray source and a flat panel detector, both from Hamamatsu, Japan. A description of the setup and its operation is reported elsewhere.<sup>[17]</sup> Three-dimensional (3D) reconstruction of the data was carried out using the commercial software “Octopus”. After reconstruction, the commercial software “VGStudioMax 1.2.1” was used to extract 3D images. For quantitative analyses such as cell size distribution and cell circularity a minimum of five 2D image slices were analyzed for each foam using the software “Image-J 1.43”. For cell circularity, all individual values are shown in the corresponding plot.

### 3. Results

Figure 2 (a-d) shows X-ray tomographic cross sections of the foams produced in this study and Fig. 3 (a-d) gives their corresponding cell size distributions and cell circularities as a function of their equivalent diameter. In all cases, the foams expanded well and filled the tube. Both the macrostructures and the pore size distribution plots (Figs. 2 and 3) show that pure aluminium and AlMg5 foamed without particles exhibit a wider cell size distribution (up to 4 – 5 mm) than AlMg5 and AlSi9Mg5 alloy foams containing particles (up to 2.5 – 3.5 mm). On the other hand, the alloy foams both with and without particles show wider cell shape distributions as expressed by circularity and also contain more finer cells than the pure aluminium foam. AlMg5 and AlSi9Mg5 alloy containing 5 vol.% of SiO<sub>2</sub> particles and pure Al foam all have about 80% porosity. The measured pore volume ( $V_p$ ) for foams in pct. is given in table 1

### 4. Discussion

#### 4.1 Hydrogen content of the melt

The gas that drives the foaming process is hydrogen first dissolved in the melt that then precipitates during pressure and temperature reduction. In the following, we estimate the amount of gas that is available for bubble formation. According to Sieverts's law the solubility of hydrogen in molten aluminium alloys is related to the partial pressure of hydrogen. The solubility  $S_{H(RP)}$  at a particular reduced pressure  $P_{RP}$  is related to the corresponding quantity at atmospheric pressure  $P_{atm}$  by

$$\frac{S_{H(atm)}}{S_{H(RP)}} = \sqrt{\frac{P_{atm}}{P_{RP}}}, \quad (1)$$

where  $S_{H(atm)}$  is the solubility of hydrogen in molten aluminium at ambient pressure defined as the gas volume per unit mass of metal.

The gas volume  $V_1$  that precipitates from the melt at reduced pressure can be written using Eq. (1):

$$V_1 = M \times (S_{H(atm)} - S_{H(RP)}) = M \times S_{H(atm)} \left( 1 - \sqrt{\frac{P_{RP}}{P_{atm}}} \right) \quad (2)$$

where,  $M$  is the mass of the metal. According to the gas law, the effective volume  $V_2$  is

$$V_2 = V_1 \left[ \frac{T_2}{T_1} \times \frac{P_{atm}}{P_{RP}} \right], \quad (3)$$

where  $T_2$  is the elevated temperature as discussed later.

Combining Eqs. 2 and 3 we obtain the total volume of precipitating gas that can form bubbles in our melt

$$V_2 = M \times S_{H(atm)} \left( 1 - \sqrt{\frac{P_{RP}}{P_{atm}}} \right) \times \left[ \frac{T_2}{T_1} \times \frac{P_{atm}}{P_{RP}} \right] \quad (4)$$

Using Wagner's interaction parameters derived from the data on hydrogen solubility in binary aluminium alloy systems <sup>[18,19]</sup> the hydrogen solubility in our molten AlMg5, AlSi9Mg5 and pure Al (99.99%) at their respective melt temperatures are calculated and given in Table 1.

#### 4.2 Reduced-pressure foaming principle

In the previous section we have shown that upon reducing pressure a part of the dissolved hydrogen precipitates from the melt. This gas generates bubbles in the melt

and leads to foam. The aforementioned results show the possibility of foaming pure aluminium and aluminium alloys without adding a blowing agent or injecting gas. The principle of RPF is schematically shown in Fig. 4. As the molten superheated metal is transported to the foaming tube and the volume gets sealed a low pressure is established instantaneously due to the continued suction of the pump which results in hydrogen precipitation from the melt. Gas precipitation causes bubble nucleation followed by growth until solidification. Although the second and third steps in Fig. 4 are shown separately they actually occur concurrently. The foam expands and fills the foaming tube, after which it rapidly solidifies due to the contact with the cold tube wall.

Our reduced-pressure foaming method is analogous to the reduced-pressure tests carried out in foundries. Standard RPT are conducted at pressures ranging from 60 to 130 mbar. It was reported that the porosities in the samples are doubled if the pressure further decreases to 33 mbar <sup>[14]</sup> without a change in the gas content in the liquid. Further, a ten fold increase in the porosity can be achieved if the pressure is decreased to below 2 to 6 mbar, indicating the pressure sensitivity of the experiment <sup>[11]</sup>. This points towards the possibility of foaming molten aluminium alloy containing only dissolved gas by strongly reducing pressure. However, care needs to be taken to avoid the loss of hydrogen from the surface of the molten metal during the time taken to pump down to these low pressures. Pressure reductions in the RPF apparatus are achieved quickly (from 1 bar to 0.2 mbar in 5 s) due to the small volume of the foaming tube. In this way, most of the dissolved hydrogen gas is completely utilised for foaming instead of being lost.

Foams are usually stabilised by adding solid particles such as SiC or oxides to the melt <sup>[1,20]</sup>. Such particles adhere to the gas/liquid interfaces and prevent coalescence of

bubbles that start to touch each other. The second characteristic feature of our foaming device is the way of preventing coalescence, namely by a very fast solidification that freezes the foamed structure before rupture of films can occur. The foaming tube is kept at room temperature, which is why the liquid foam cools down rapidly at a rate of 35 K/s and gas losses from the surface of the liquid foam by diffusion are reduced. Excessive losses would cause foam collapse since there is no continuous gas production to compensate such losses as it is when a blowing agent like  $\text{TiH}_2$  is used [21]. Slow solidification would also cause the bubbles to float to the surface of the melt and rupture, especially for the alloys that contain no stabilizing particles [14]. Too fast cooling of the tube would freeze the melt before it foams and fills the tube. To avoid this, the alloys were superheated before pouring into the apparatus, i.e. to 150 K above the melting point. The arrangement of sucking the molten metal into the foaming tube and self-sealing the tube after minimises the delay in transporting the molten metal into the tube. Such delay would cause a temperature drop of the melt and hence gas precipitation and loss before foaming. The effect of fast cooling combined with gas out-diffusion gives rise to a thick outer surface at the bottom of the pure aluminium foam, see Fig. 2 (a). Alloy AlMg5 or AlSi9Mg5 foams, see Fig. 2 (b-d), with and without particles do not show any such thick outer surface because the gap between their liquidus and solidus temperatures (35 K for AlMg5 and 46 K for AlSi9Mg5) allows for pore formation during solidification.

In our foaming process the hydrogen dissolved in the molten superheated aluminium alloys at atmospheric pressure is precipitated by dynamically reducing the ambient pressure. The amount of dissolved gas in the melts is not known at present and there is also no information about its distribution. It seems justified to assume that stirring the melt for particle addition and/or the turbulence during flow at high

velocity into the foaming tube helps in distributing the dissolved gas homogeneously [11]. To estimate the amount of gas precipitating under constant reduced pressure, complete saturation with hydrogen,  $S_{H(am)}$ , at the melt temperatures and at ambient pressure is first considered, see Table 1. As in reality, molten pure aluminium dissolves only ~20% of this value irrespective of its melting temperature [22] we use this estimate in a second scenario and recalculate the hydrogen content in our alloys to the value given in Table 1 in the 5<sup>th</sup> column.

The pressure reduction applied during foaming is dynamic and therefore it is difficult to measure the exact or effective reduced pressure  $P_{RP}$ , of foaming. However, it can be back-calculated using the measured pore volume of the foams and the hydrogen solubility in the melt without considering the amount of gas lost by out-diffusion. The measured pore volume  $V_p$  is equal to  $V_2$  in Eq. 4. The effective reduced pressure  $P_{RP}$  is calculated using Eq. 4 and the procedure for the calculation is given in the Appendix.

It should be noted that the temperature  $T_2$  is considered to be the liquidus temperature of the alloy or the melting point of the metal, considering the shrinkage of gas pores in the liquid foams. The reduced pressure necessary to produce a pore volume  $V_p$ , in foams both assuming complete solubility of hydrogen and 20% of its solubility limit in molten aluminium was calculated and is given in Table 1. It can be seen that the pressure reduction required is much higher for foaming aluminium and aluminium alloy melts that contain only 20% of dissolved gas than for fully saturated melts. Since our apparatus can reach 0.2 mbar in 5 seconds it was possible to foam aluminium alloy melts even though they might have contained less hydrogen than the saturation level.

## 5.2 Nucleation of bubbles

No stable foams have been produced from aluminium or its alloys in the absence of stabilizing particles through any of the existing traditional liquid-route foaming processes. A certain volume fraction of particles is required to obtain sufficiently stabilised foams [23] in the course of standard foaming under normal conditions where the foaming time is in the range of several minutes. In RPF, faster solidification of the liquid foam is the reason for obtaining stable foams without added particles. However, the polyhedral cell shapes with pronounced cell walls and plateau borders observed in the pure aluminium and AlMg5 foams, see Fig.2 (a) and (b), indicate that even these foams are stabilised [24]. It is suspected that oxide inclusions that form during melting or are entrained during the occasional melt stirring contribute to stabilisation in pure aluminium and AlMg5 foams to which no extra particles have been added.

Nucleation of pores occurs primarily at heterogeneous sites [25]. The heterogeneous sites are the oxide inclusions and/or SiO<sub>2</sub> particles in our foams. Samuel and Samuel [14] show that oxide inclusions in a melt trap pores and prevent them from escaping through the melt surface when it was under reduced pressure. These oxide inclusions can significantly increase the porosity even if the hydrogen content is low.

The Gibbs free energy of heterogeneous nucleation of a bubble in a liquid is given by [26,27]

$$\Delta G^*_{het} = \frac{16\pi\gamma_{Bl}^3}{3\Delta P^2} \times f(\theta), \quad (7)$$

where  $\Delta G^*_{het}$  is the Gibb's free energy for heterogeneous nucleation of a bubble in a liquid,  $\gamma_{Bl}^3$ , is the surface energy of the bubble-liquid interface and

$$\Delta P = P_B - P_l,$$

where  $P_B$  and  $P_l$  are the pressures inside the bubble and the metallostatic pressure, respectively, and

$$f(\theta) = \left(\frac{1}{4}\right)(2 - \cos \theta)(1 + \cos \theta)^2, \quad (8)$$

where  $\theta$  is the contact angle between the stabilizing particle/inclusion and the gas (measured on the gas side), see Fig.5.

$$P_B - P_l = \frac{2\gamma_{Bl}}{R}, \quad (9)$$

where  $R$  is the radius of curvature of the bubble [27]. Thus we obtain

$$\Delta G^*_{het} = \frac{4}{3}\pi\gamma_{Bl} \times R^2 \times f(\theta). \quad (10)$$

Figure 5 shows the schematic of bubble nucleation at the solid-liquid interface. The radius of curvature  $R$  can be derived using the radius of nuclei,  $r$  and the contact angle  $\theta$ .

According to Eq. 10 the free energy required to nucleate a bubble decreases with the contact angle of the particles. The contact angle of  $Al_2O_3$  (oxide inclusion) is  $\theta = 93^\circ$  in molten aluminium at  $850^\circ C$  [28]. Then  $f(\theta)$  calculated using Eq. 8 is 0.46. Similarly, the contact angle for  $SiO_2$  is  $120^\circ$  in molten aluminium at  $750^\circ C$  [29] and the corresponding  $f(\theta)$  value is therefore 0.15. This shows that in the presence of  $SiO_2$ , bubbles will nucleate at  $SiO_2$  and not at  $Al_2O_3$  particles.

## 6. Summary

- A reduced-pressure foaming (RPF) technique for the production of aluminium and aluminium alloy foams was developed.
- Foaming was done by precipitating and expanding hydrogen gas initially dissolved in the molten alloy that is released by reducing both pressure and temperature.

- The gas dissolved in the melt could be utilised for foaming by minimizing the delay in melt transportation to the foaming chamber, attaining reduced pressure and providing stabilisation by quickly solidifying the liquid foam.
- The foaming method proposed here allows us to lower the pressure to well below the values required for foaming aluminium alloy melts containing 20% of the maximum hydrogen content.
- Pure aluminium (99.99% purity), AlMg5 alloy without particles and AlMg5 or AlSi9Mg5 alloys containing 5 vol.% of SiO<sub>2</sub> particles were successfully foamed to 80 % porosity. The cell structure was uniform as shown by computer tomography.

**Acknowledgement:** The authors would like to thank Dr. André Hilger for the X-ray computed tomography of the foam samples

## References

1. J. Banhart: *Prog. Mater. Sci.*, 2001, vol. 46, pp. 559-632.
2. T. Miyoshi, M. Itoh, S. Akiyama and A. Kitahara: *Adv. Eng. Mater.*, 2000, vol. 4, pp. 179-183.
3. V. Gergely and B. Clyne: *Adv. Eng. Mater.*, 2000, vol.2, pp. 175-178.
4. G. S. Vinod Kumar, M. Chakraborty, F. Garcia-Moreno and J. Banhart: *Metall. Mater. Trans. A*, 2011, vol.42, pp. 2898-2908.
5. J. D. Bryant, M. Crowley., W. Wang, D. Wilhelmy and J. Kallivayalil: Porous metal and metallic foams, p.19, DEStech Publication Inc., Pennsylvania, 2007.
6. V. Gergely, D.C. Curran, and T.W. Clyne: *Compos. Sci. & Technol.*, 2003, vol.63, pp. 2301-2310.
7. D. Leitlmeier, H.P. Degischer, and H.J. Flankl: *Adv. Eng. Mater.*, 2002, vol.4, pp. 735-740.
8. N. Babcsán, D. Leitlmeier, H.P Degischer and J. Banhart: *Adv. Eng.Mater.*, 2004, vol.6, pp. 421-428.
9. V. Shapalov, Porous and cellular materials for structural applications, vol.512, p. 281, MRS publication, Warrendale, 1998.
10. H. Nakajima: *Prog. Mater. Sci.*, 2007, vol. 52, pp. 1091-1173.
11. J.Campbell: *Castings*, 2<sup>nd</sup>ed., Butterworth-Heinmann, Burlington, 2003
12. W. La-Orchan: Ph.D. Thesis, McGill University, Montreal, Canada, 1994.
13. G. S. Vinod Kumar and Suresh Sundarraj: *Metall. Mater. Trans. B*, 2010, vol.41, pp. 495-499.
14. A. M. Samuel, and F.H. Samuel: *Metall. Mater. Trans. A*, 1993, vol.24, pp. 1857-1868.
15. K. Renger, and H. Kaufmann: *Adv.Eng. Mater.*, 2005, vol.7, pp. 117-123.

16. H. Wiehler, C. Körner and R.F. Singer: *Adv. Eng. Mater.*, 2008, vol.10, pp. 171-178.
17. J. Banhart: *Advanced Tomographic Methods in Materials Research*, Oxford University Press, 2008.
18. P. N.Anyalebechi: *Scripta Metall. Mater.*, 1995. vol.33, pp. 1209-1216.
19. P. N.Anyalebechi: *Scripta Mater.*, 199, vol.34, pp. 513-517.
20. S. W. IP, Y.Wang, and J. M. Toguri: *Can. Metall. Q.*, 1999, vol. 38, pp. 81-92
21. M. Mukherjee, F. Garcia-Moreno, and J. Banhart: *Acta Mater.*, 2010, vol.58 pp. 6358-6370.
22. D.E. J. TALBOT: *The Effects of Hydrogen in Aluminium and its Alloys*, Maney Publishing, London, 2004.
23. O.Prakash, H. Sang and J.D. Embury: *Mater. Sci. Eng. A*, 1995, vol.199, pp. 195-203.
24. C. Körner, M. Hirschmann, V. Bräutigam and R.F. Singer: *Adv. Eng. Mater.*, 2004, vol.6, pp. 385-390.
25. P. Mohanty, F. Samuel and J. Gruzleski: *Metall. Mater. Trans. A*, 1993, vol.24, pp. 1845-1856.
26. J.S. Colton and N.P. Suh: *Polym. Eng. Sci.*, 1987, vol.27, pp. 500-503.
27. M.Blander, and J.L. Katz, *AIChE J.*, 1975, vol.21, pp. 833-848.
28. V. Laurent, D. Chatain, C. Chatillon and N. Eustathopoulos: *Acta Metall.*, 1988, vol.36, pp. 1797-1803.
29. V. Laurent, D. Chatain and N. Eustathopoulos: *Mater. Sci. Eng. A*, 1991, vol.135, pp. 89-94.

## Appendix

For calculating the reduced pressure  $P_{RP}$  we consider that  $P_{atm} = 1$  bar and define

$$P'_{RP} = \frac{P_{RP}}{P_{atm}}$$

Rearranging Eq.(4) gives

$$V_2 \times \frac{1}{M} \times \frac{1}{S_{H(atm)}} \times \frac{T_1}{T_2} = (1 - \sqrt{P'_{RP}}) \times \frac{1}{P'_{RP}} \quad , \quad (4a)$$

or

$$\left( V_2 \times \frac{1}{M} \times \frac{1}{S_{H(atm)}} \times \frac{T_1}{T_2} \right) \times P'_{RP} + \sqrt{P'_{RP}} - 1 = 0 \quad , \quad (4b)$$

which is a quadratic equation of type  $ax^2 + bx + c = 0$  with coefficients

$$a = \left( V_2 \times \frac{1}{M} \times \frac{1}{S_{H(atm)}} \times \frac{T_1}{T_2} \right), \quad b = 1, \quad c = -1 \quad \text{and} \quad x = \sqrt{P'_{RP}}$$

and has the solutions

$$P'_{RP} = x^2 = \left( \frac{-b \pm \sqrt{b^2 - 4ac}}{2a} \right)^2 \quad (4c)$$

The  $P_{RP}$  calculated from Eq.4c has two solutions due to +ve and -ve signs in equation. Both the solutions are given in table 1 at 7<sup>th</sup> and 8<sup>th</sup> columns.

## List of Figures

Fig.1 Setup used for reduced-pressure foaming.

Fig.2 X-ray tomographic reconstruction of (a) Al (99.99% pure), (b) AlMg5, (c) AlMg5 + 5 vol.% SiO<sub>2</sub> and (d) AlSi9Mg5 + 5 vol.% SiO<sub>2</sub> foams. SiO<sub>2</sub> was applied as microsilica particles of average size 44 μm. The melt temperature before pouring into the foaming apparatus was 850 °C for pure Al and 750 °C for all the alloys.

Fig.3 Cell size distribution and circularity vs. equivalent diameter of cells in (a) Al (99.99% pure), (b) AlMg5, (c) AlMg5 + 5 vol.% SiO<sub>2</sub>, (d) AlSi9Mg5 + 5 vol.% SiO<sub>2</sub> foams. The upper axis has been reversed to avoid overlap of data.

Fig.4 Steps occurring during reduced-pressure foaming.

Fig.5 Schematic of a gas bubble at a solid –liquid interface. Here, the solid is the heterogeneous nucleation site.

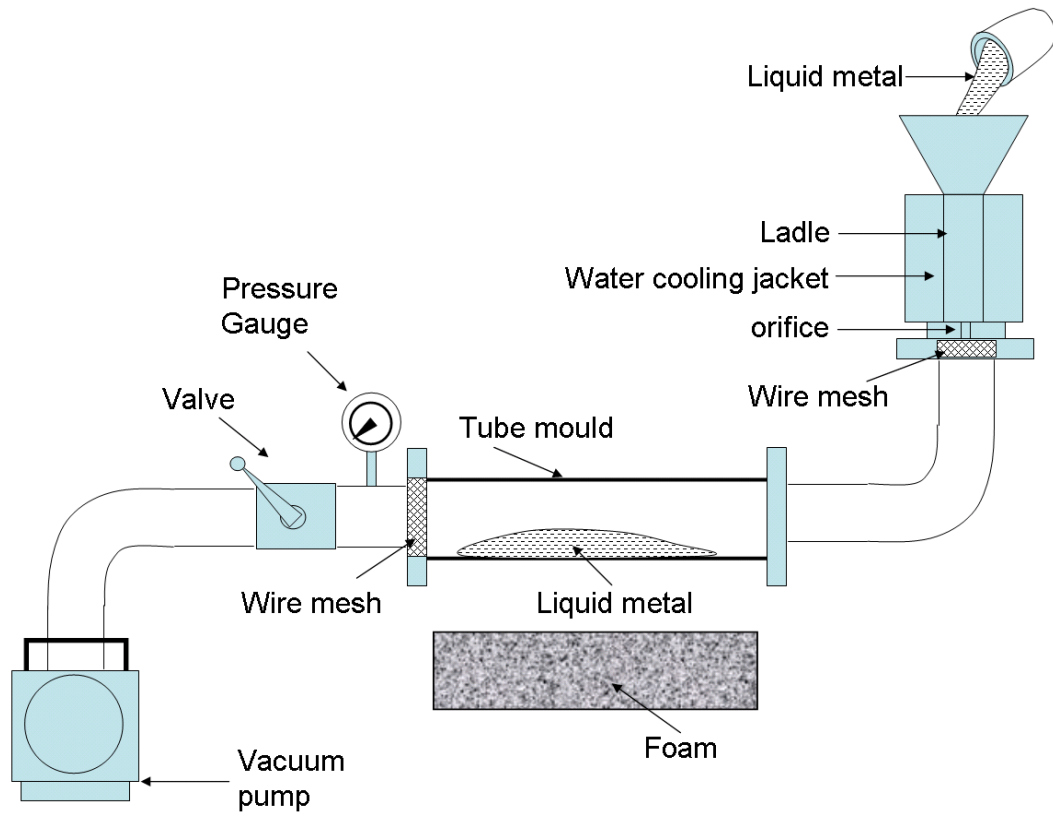


Fig.1. Setup used for reduced-pressure foaming .

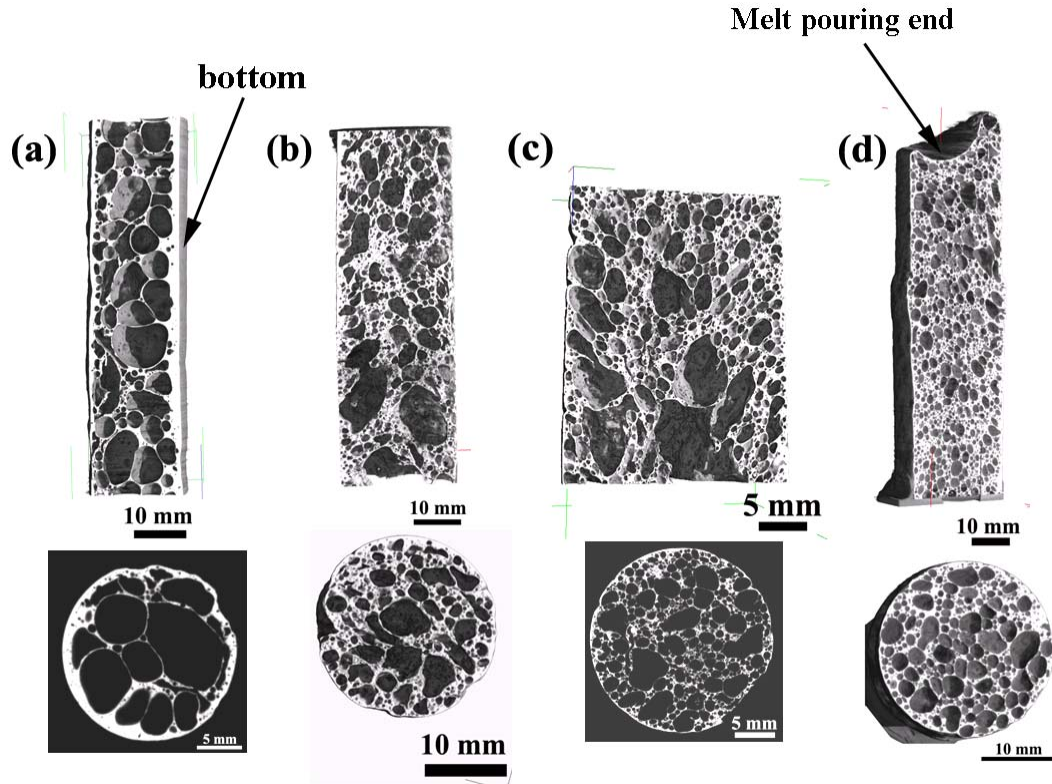


Fig.2. X-ray tomographic reconstruction of (a) Al (99.99% pure), (b) AlMg5, (c) AlMg5 + 5 vol.% SiO<sub>2</sub> and (d) AlSi9Mg5 + 5 vol.% SiO<sub>2</sub> foams. SiO<sub>2</sub> was applied as microsilica particles of average size 44 μm. The melt temperature before pouring into the foaming apparatus was 850 °C for pure Al and 750 °C for all the alloys.

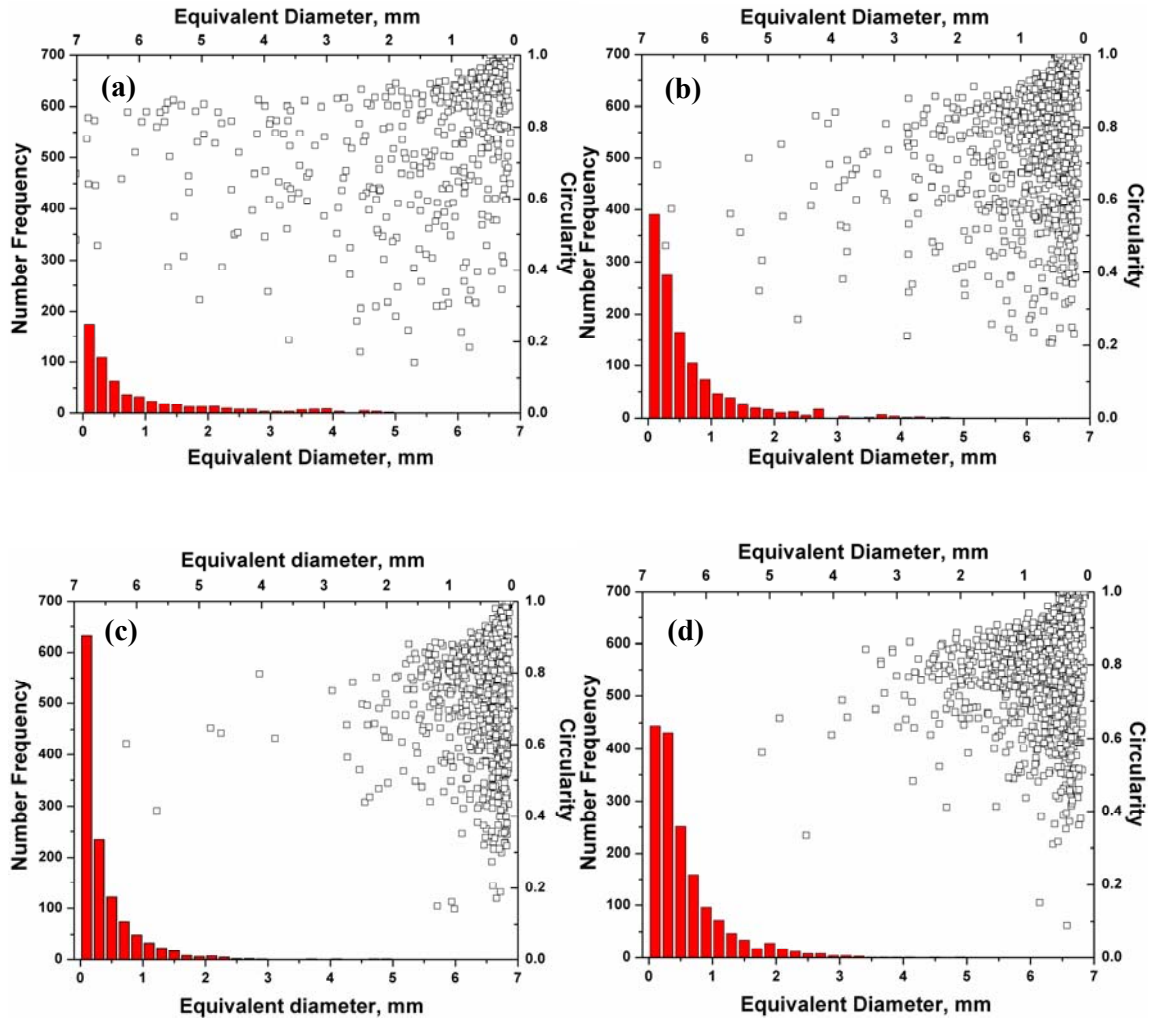


Fig.3. Cell size distribution and circularity vs. equivalent diameter of cells in (a) Al (99.99% pure), (b) AlMg5, (c) AlMg5 + 5 vol.% SiO<sub>2</sub>, (d) AlSi9Mg5 + 5 vol.% SiO<sub>2</sub> foams. The upper axis has been reversed to avoid overlap of data.

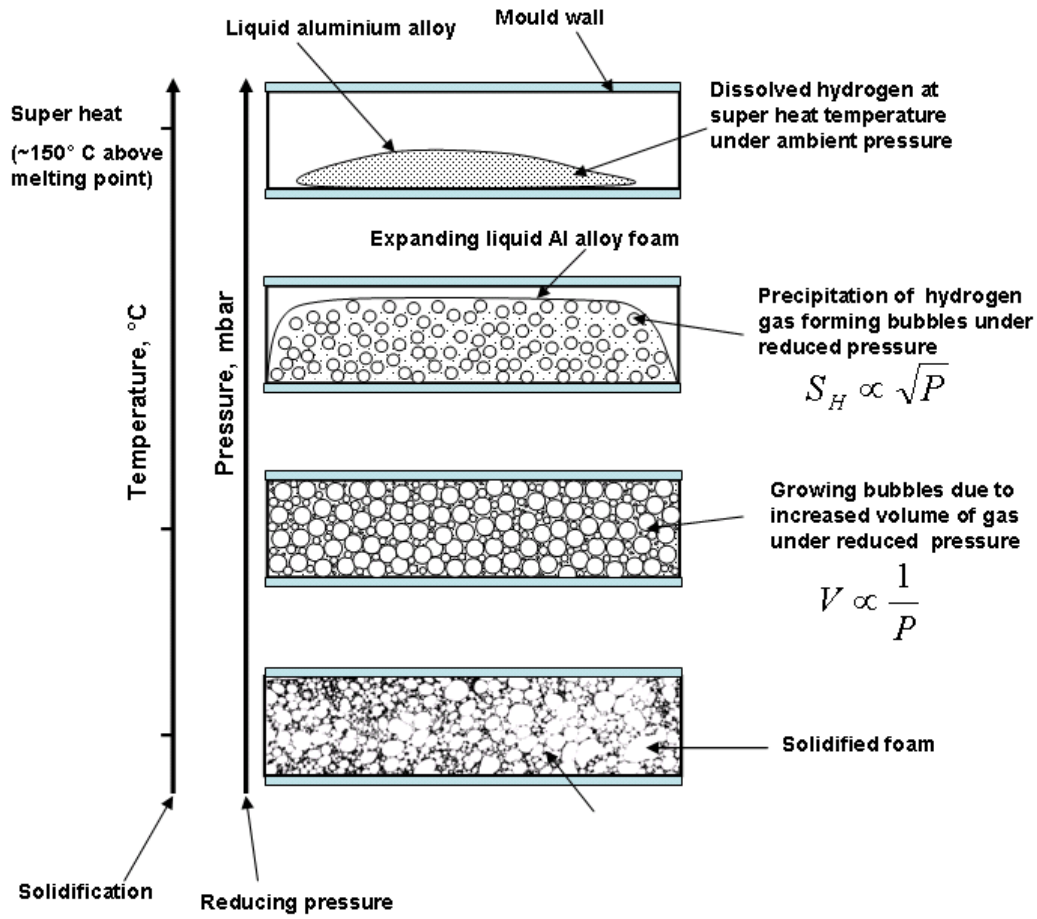


Fig.4. Steps occurring during reduced-pressure foaming.

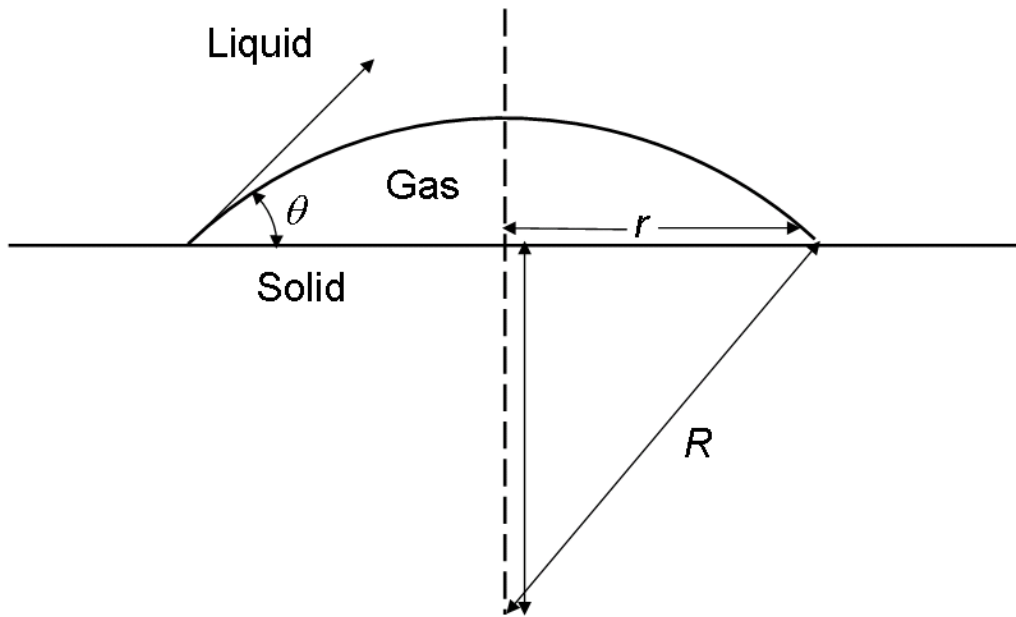
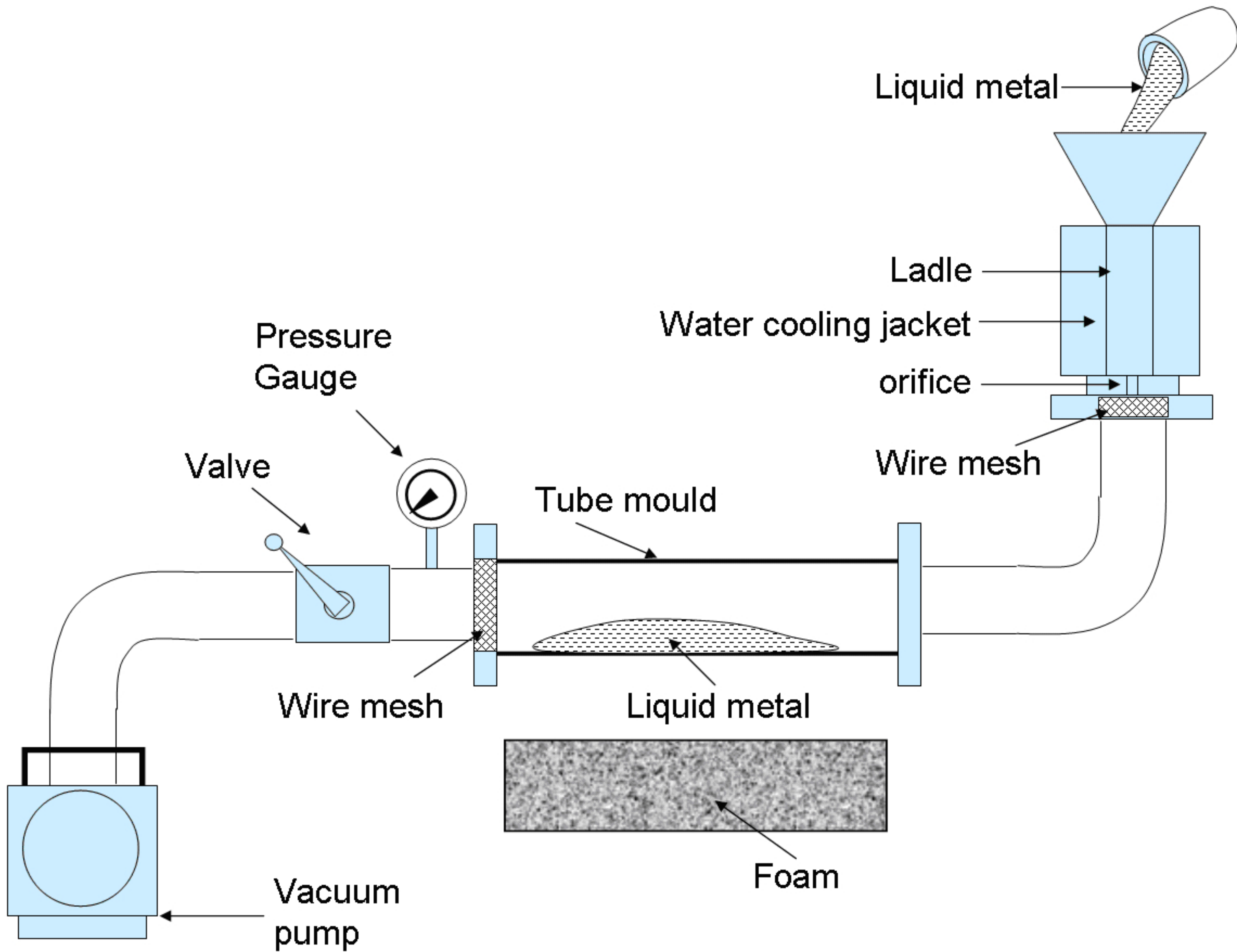


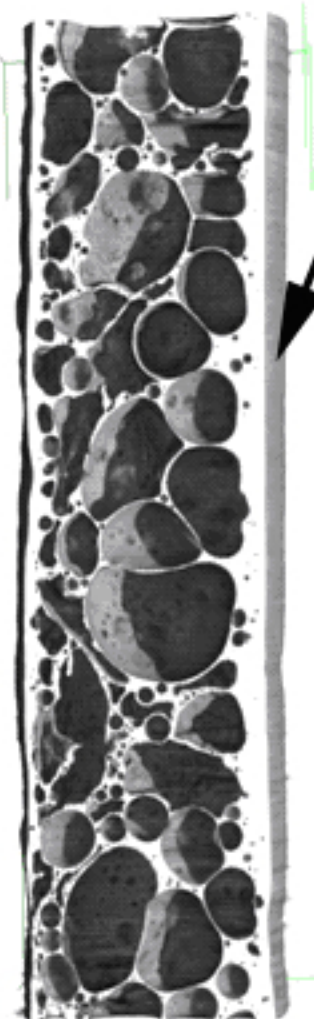
Fig.5. Schematic of a gas bubble at a solid –liquid interface. Here, the solid is the heterogeneous nucleation site.



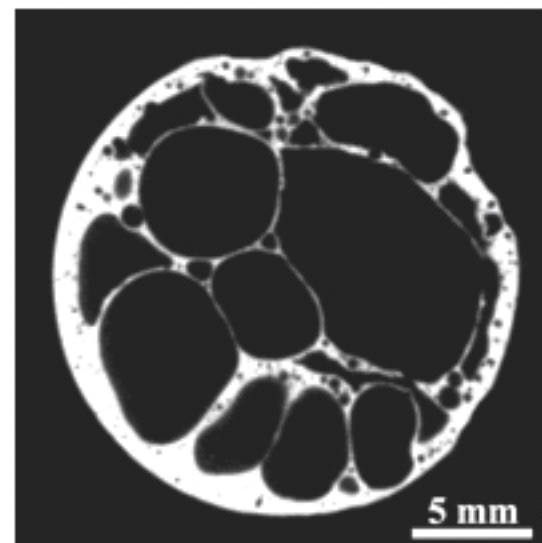
Melt pouring end

bottom

(a)

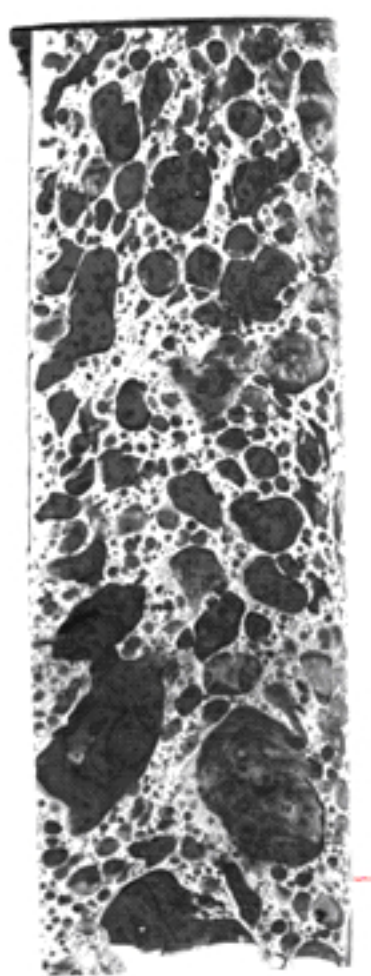


10 mm

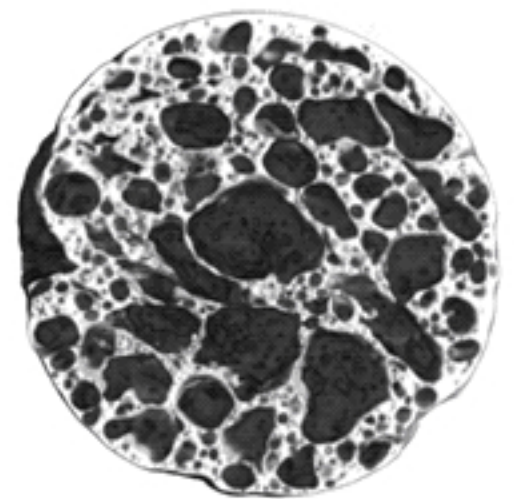


5 mm

(b)

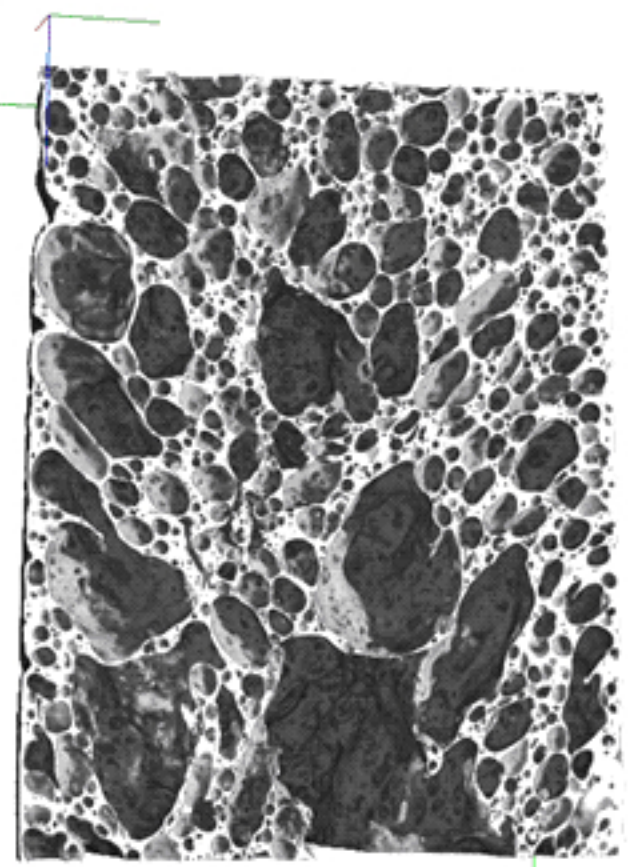


10 mm

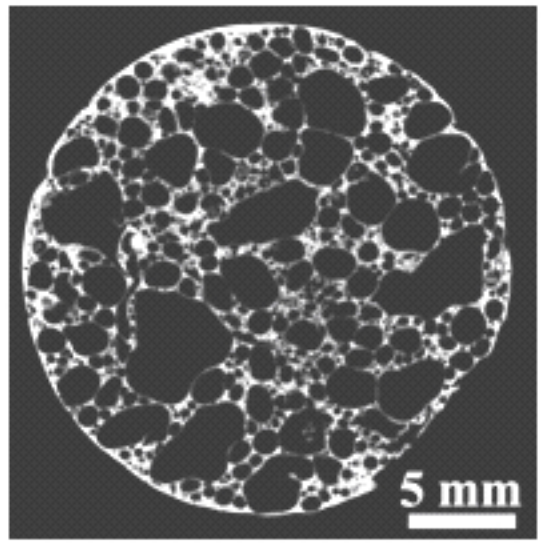


10 mm

(c)

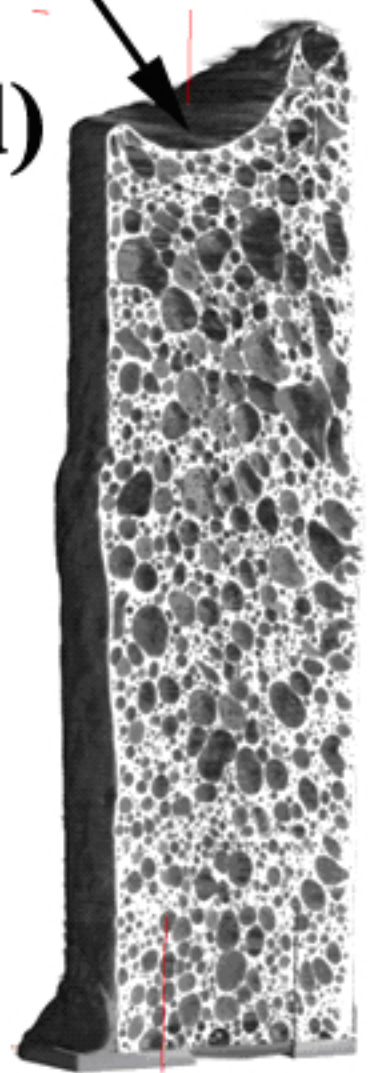


5 mm

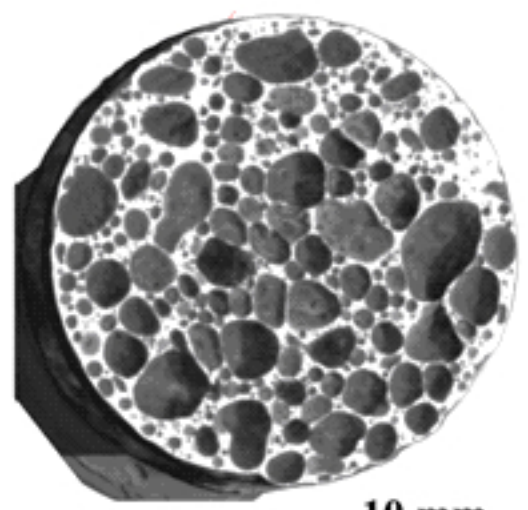


5 mm

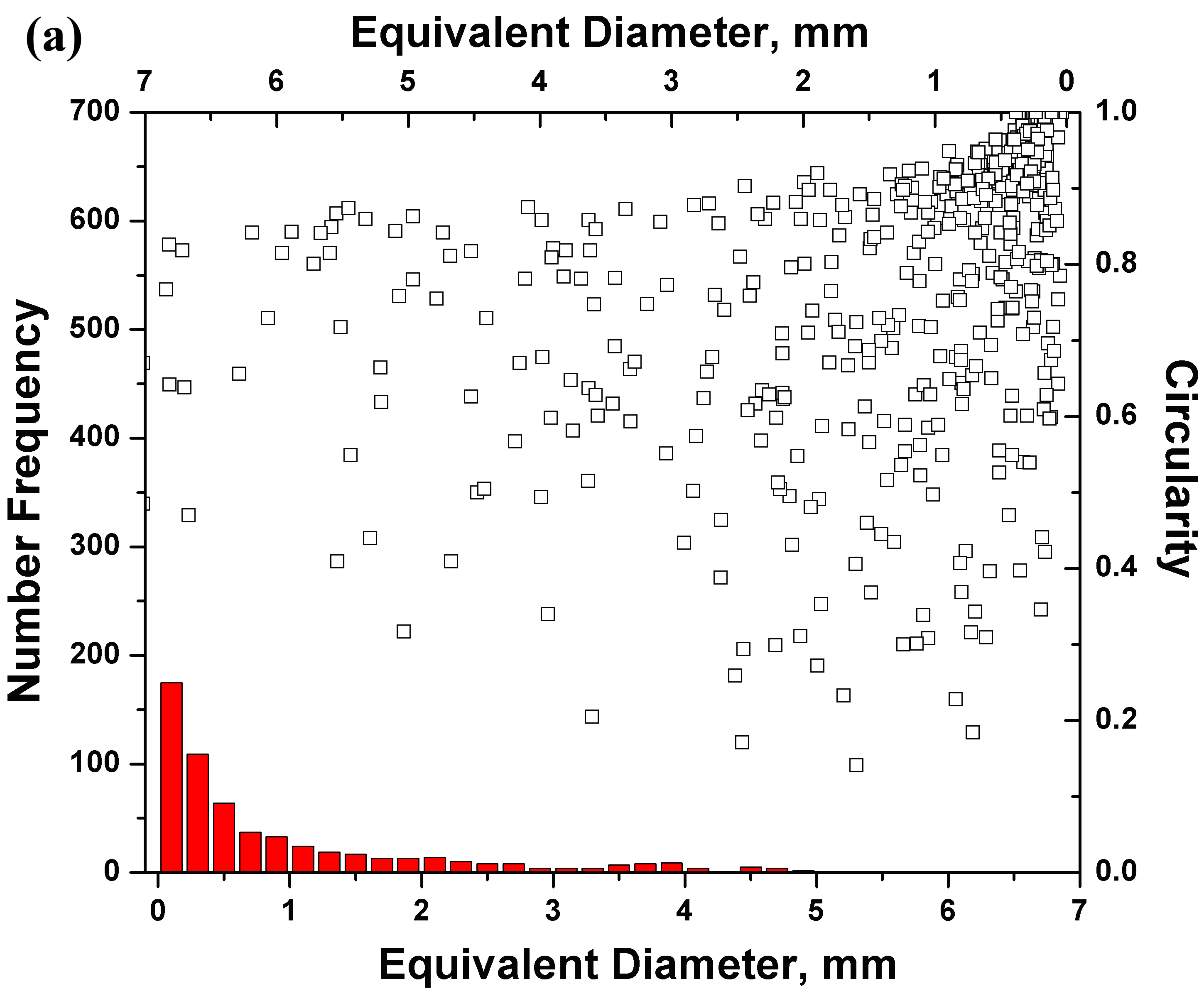
(d)

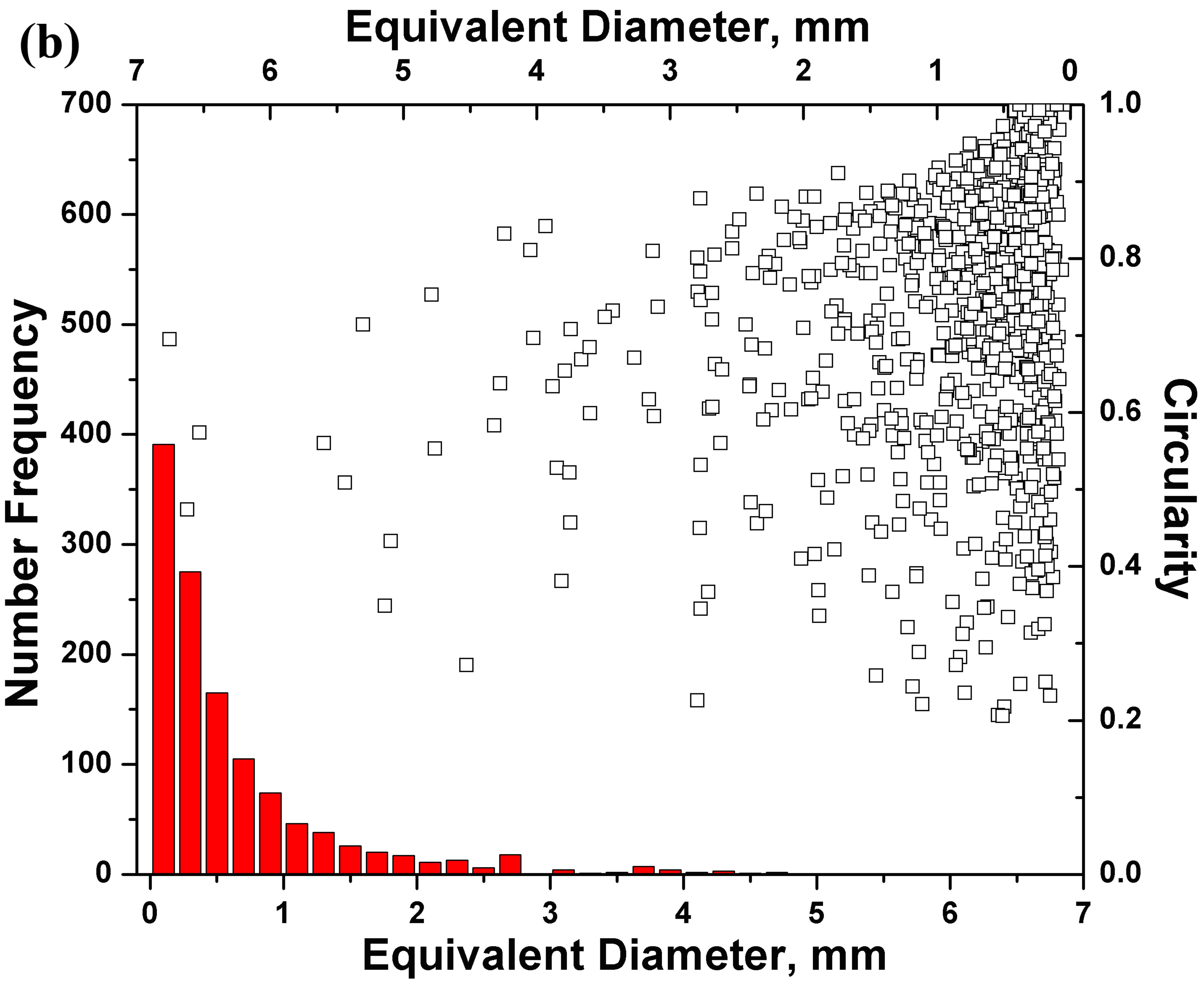


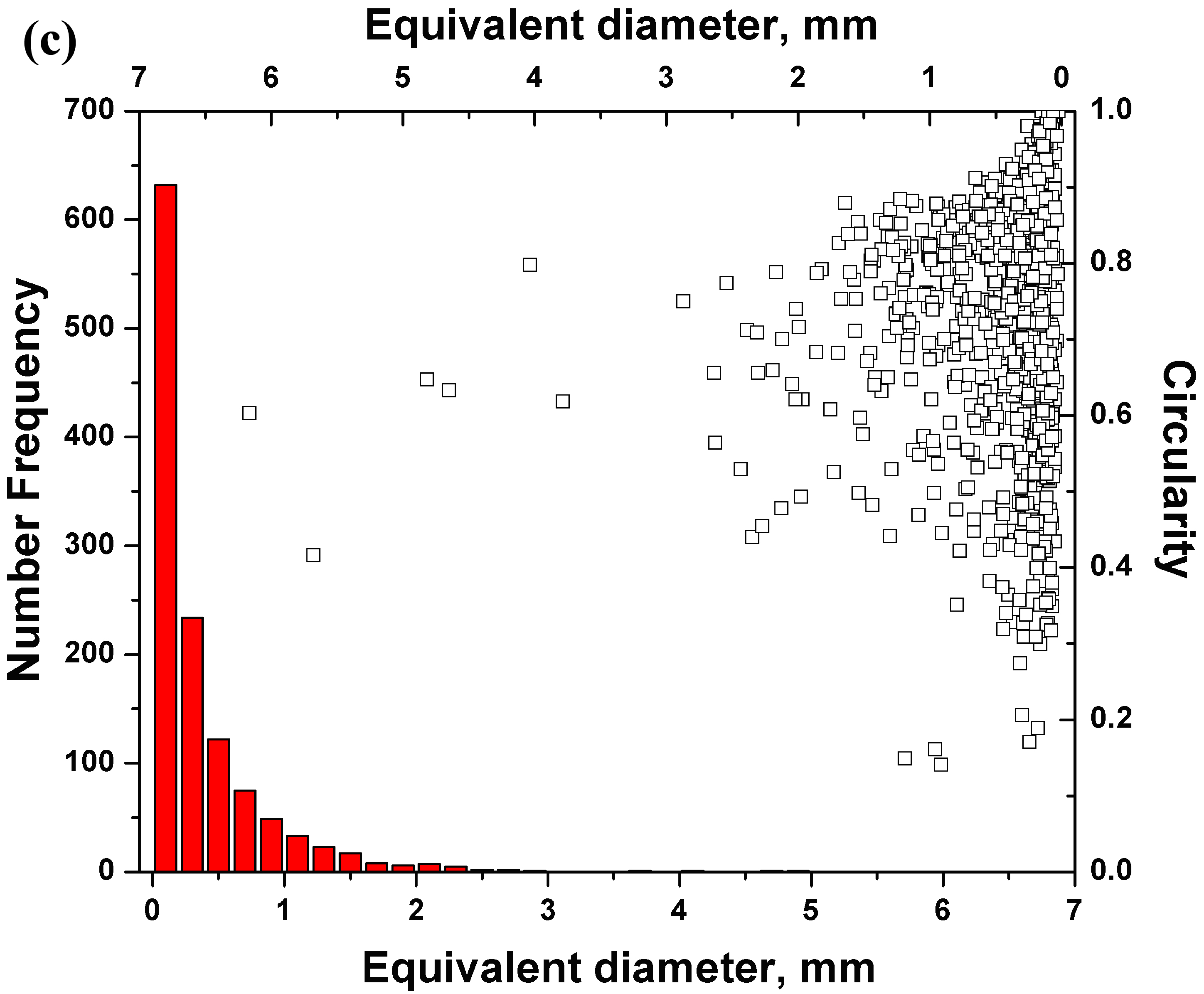
10 mm

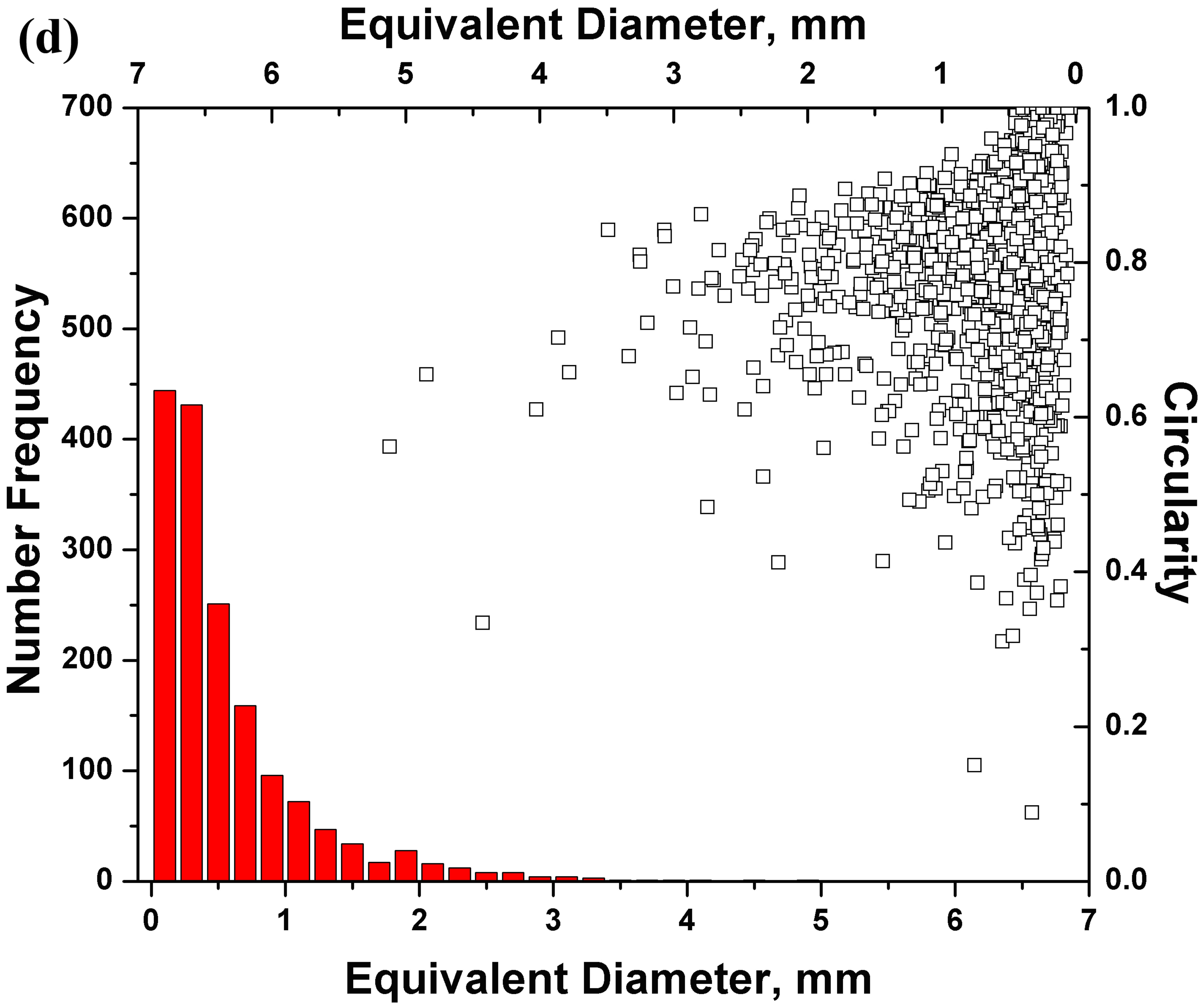


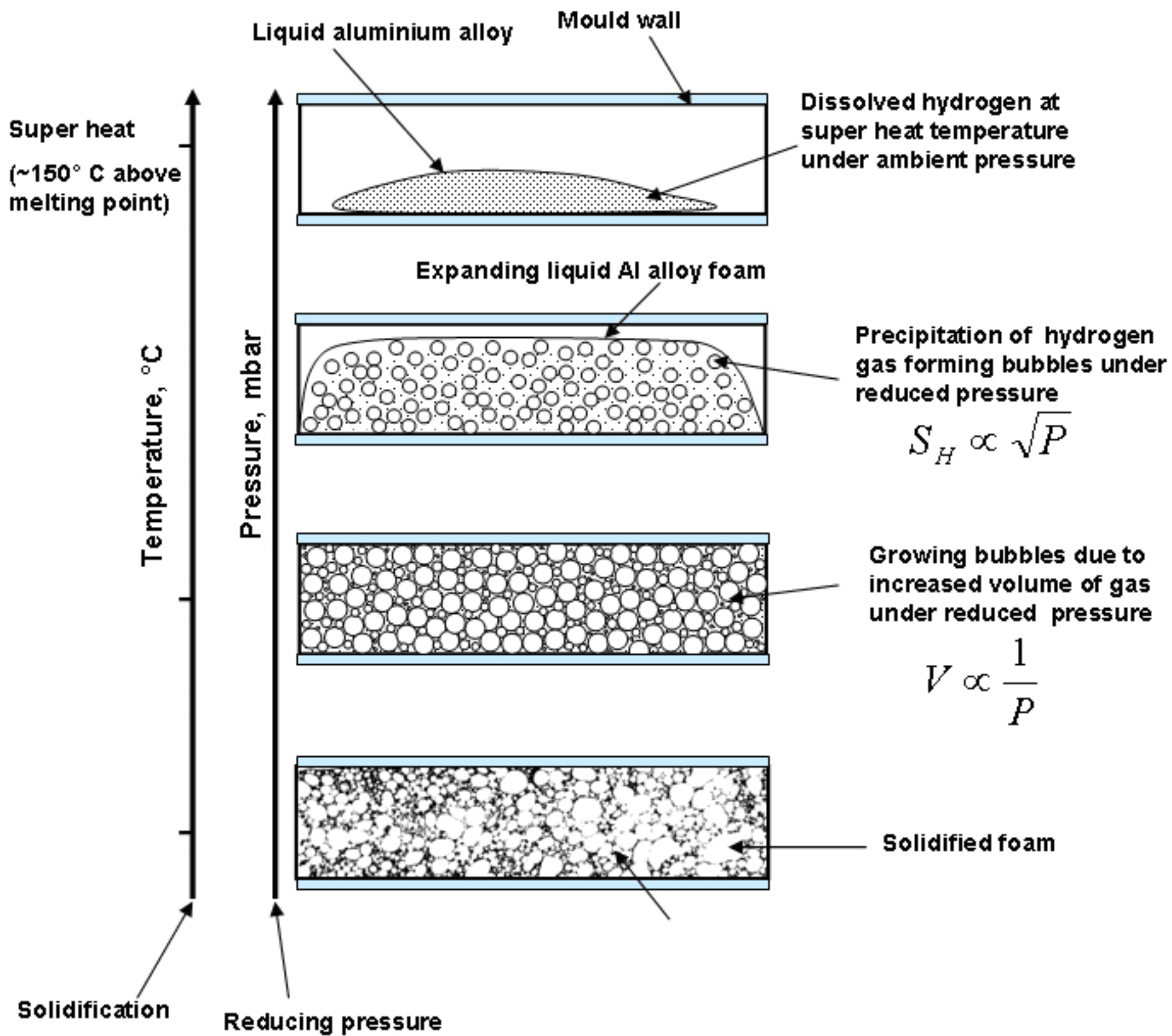
10 mm











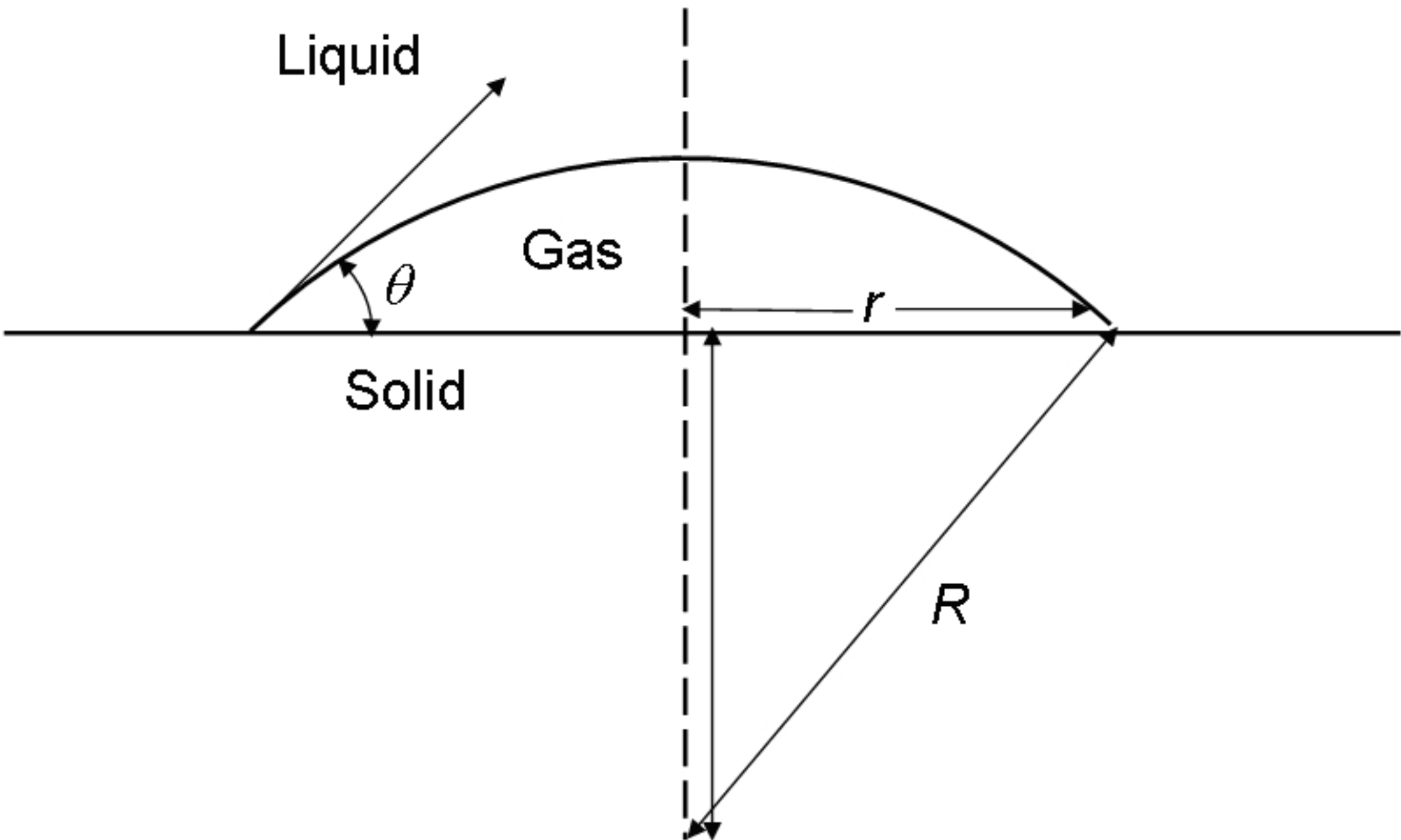


**Table1.** Details of the alloys used for foaming, their hydrogen solubility, the measured pore volume fraction, and the calculated reduced pressure. In the column 7 and 8 the  $P_{RP}$  values given in parenthesis is the second solution (- ve sign) of the Eq.4c.

alloy	Particle content (vol.% SiO <sub>2</sub> )	melt pouring temperature, (°C)	$S_{H(atm)}$ @ melt pouring temperature @ 1013 mbar (ml/g)	Hydrogen content considering only 20% of gas solubility (ml/g)	$V_p$ , measured pore volume in foams (vol.%)	$P_{RP}$ , calculated reduced pressure considering complete solubility (mbar)	$P_{RP}$ , calculated reduced pressure considering 20% solubility (mbar)
Al (99.99%)	none	850	$0.57 \times 10^{-2}$	$0.114 \times 10^{-2}$	81	10 (12)	2 (2)
AlMg5	5	750	$2.63 \times 10^{-2}$	$0.526 \times 10^{-2}$	83	36 (54)	8 (9)
AlMg5	none	750	$2.63 \times 10^{-2}$	$0.526 \times 10^{-2}$	not measured	36 (54)	8 (9)
AlSi9Mg5	5	750	$1.95 \times 10^{-2}$	$0.39 \times 10^{-2}$	80	32 (48)	7 (8)